Power-Demand Driven Modeling: A Universal Data-Driven Circuit Framework for Diverse Photovoltaic Technologies

Aaron Shmaryahu
Electrical and electronics engineering
Ariel University
Ariel, Israel
aaron.shmaryhu@msmail.ariel.ac.il

Roni Zakay
Electrical and electronics engineering
Ariel University
Ariel, Israel
ronie@ariel.ac.il

Ilan Aharon
Electrical and electronics engineering
Ariel University
Ariel, Israel
https://orcid.org/0000-0003-1382-7587

Abstract*— Accurate real-time power forecasting and source modeling are critical for the stable operation of modern smart grids. Existing modeling frameworks are typically source-specific and rely heavily on terminal voltage dynamics rather than direct power demand, creating a functional gap in real-time load-power balancing. To address these limitations, this paper presents a novel Universal Data-Driven Circuit Model (UDCM) designed for the unified representation of diverse photovoltaic (PV) technologies. The UDCM features a source-agnostic architecture that utilizes n-dimensional interpolation and extrapolation of experimental data, successfully replacing rigid physical equations with a flexible mapping system. Uniquely driven by real-time load power demand (P_{demand}), the model directly maps fluctuating load requirements to the source's electrical output through deterministic, non-iterative calculations, thereby eliminating high computational overhead. Empirical validation using both monocrystalline and polycrystalline PV modules under untested environmental conditions demonstrates high-fidelity tracking of physical measurements. The proposed model achieves an absolute percentage error (APE) below 1.4% and a coefficient of determination (R^2) of up to 0.996. Consequently, the UDCM offers a computationally efficient, robust, and scalable solution for real-time performance optimization and load balancing in modern microgrids.

Keywords*— photovoltaic cell, Universal Data-Driven Circuit Model, Smart grid, Microgrid

I. INTRODUCTION

Modern power systems are undergoing a paradigm shift toward Smart Grids, characterized by the massive integration of renewable energy sources and advanced storage technologies [1]. These grids now rely on a diverse mix of "soft" energy sources, ranging from photovoltaic (PV) systems—employing various chemical compositions and technologies such as monocrystalline and polycrystalline cells—to various types of fuel cells and battery energy storage systems [2].

A critical challenge in managing and optimizing such grids is accurately predicting the energy capacity each source can provide at any given moment [3]. Because these grids comprise a multitude of distinct technologies, each with its own unique physical and chemical characteristics, they do not exhibit uniform behavior. Consequently, each source requires a specific modeling approach to capture its precise response to environmental and operational changes [4]. Furthermore, effectively modeling energy requirements in a smart grid necessitates a focus on load power demand [5]. To maintain a stable load-power balance, grid operators must predict and manage the real-time power consumption of various loads. This ensures that the instantaneous availability of energy from various sources can meet the grid's load requirements at any given moment. Failure to accurately model this balance can lead to grid instability or inefficient energy distribution [6].

Currently, most modeling frameworks are designed for specific sources and specialized technologies [7]. While solutions for source modeling in smart grids do exist, they generally require the application of a distinct, dedicated model for each technological variant within the grid. To simulate the entire system, these disparate models must be integrated into a unified set of energy equations. This integration process significantly slows down the simulation environment and increases system complexity, making large-scale grid analysis cumbersome [8]. Moreover, a fundamental limitation of existing models is their reliance on terminal voltage dynamics. Most traditional frameworks characterize energy sources based on their voltage-current (V-I) behavior [9][10]. However, this approach does not inherently support integrating general power demand from loads, a core requirement in modern power systems. In a real-world smart grid, the primary operational driver is the fluctuating power request from the load, rather than a fixed voltage profile. The inability of current models to be directly driven by power demand creates a functional gap, complicating the task of maintaining a real-time load-power balance across the grid [11].

To overcome these limitations, this paper introduces a novel UDCM specifically tailored for the unified representation of diverse photovoltaic technologies through a source-agnostic architecture. The core innovation lies in its ability to model different types of solar cells—such as monocrystalline, polycrystalline, and thin-film—using the same circuit configuration, shifting complexity from rigid physical equations to a flexible mapping system based on n-dimensional interpolation and extrapolation. Central to this approach is a methodology explicitly driven by power demand (P_{demand}), in which the model operates independently of predefined voltage or current values by directly mapping real-time load demand and environmental factors to the source's electrical output. By intersecting the required power level with experimentally derived characteristic profiles, the UDCM identifies physically feasible operating points and enables deterministic, non-iterative calculations, providing a computationally efficient and high-fidelity solution for real-time performance optimization in modern smart grids.

XXX-X-XXXX-XXXX-X/XX/$XX.00 ©20XX IEEE

The remainder of this paper is organized as follows: Section II, details the mathematical principles and architecture of the proposed UDCM framework. Section III, presents the empirical validation and case studies for polycrystalline and monocrystalline technologies. Finally, Section IV, concludes the paper.

II. UDCM Principle

As illustrated in Fig. 1, the process begins with a structured, sequential data flow, with the Inputs block serving as the primary interface to external and environmental conditions. This block captures three critical variables that drive the entire simulation: the real-time Power Demand (P_{demand}), which defines the specific load requirements, the Source Characteristics, which provide the baseline operational parameters, and the Temperature (T), which is a vital factor influencing the physical and electrochemical behavior of the source.

The interpolation and extrapolation block serves as the "intelligence" of the model, processing raw experimental data stored in multidimensional Look-up Tables. By employing an n-dimensional linear interpolation engine, the model dynamically calculates the source voltage and current for operating points located within the predefined data grid. If the operating point falls outside the available range, the system applies linear extrapolation based on the local gradient of the nearest known grid point to ensure continuous, physically consistent estimates. The source's output voltage and current are represented in (1) and (2).

$$v_o^{stat}(n) = \begin{cases} v_o\left(x_{1b_1}, x_{2b_2}, \dots, x_{nb_n}\right) \cdot \\ \sum_{b\in\{0,1\}^n} \prod_{i=1}^{n} \left(\left(\frac{x_i^* - x_{i0}}{x_{i1} - x_{i0}}\right)^{b_i} \cdot \left(1 - \frac{x_i^* - x_{i0}}{x_{i1} - x_{i0}}\right)^{1-b_i} \right), inter. \\ v_o(near) + \sum_{i=1}^{n} (slope_i \cdot (x_i^* - x_i)), extrap. \\ V_{OC} \end{cases} \quad \begin{matrix} \\ \\ , v_o < V_{OC} \\ \\ , V_o \geq V_{oc} \end{matrix} \tag{1}$$

$$i_o(n) = \begin{cases} i_o\left(x_{1b_1}, x_{2b_2}, \dots, x_{nb_n}\right) \cdot \\ \sum_{b\in\{0,1\}^n} \prod_{i=1}^{n} \left(\left(\frac{x_i^* - x_{i0}}{x_{i1} - x_{i0}}\right)^{b_i} \cdot \left(1 - \frac{x_i^* - x_{i0}}{x_{i1} - x_{i0}}\right)^{1-b_i} \right), inter. \\ i_o(near) + \sum_{i=1}^{n} (slope_i \cdot (x_i^* - x_i)), extrap. \\ I_{SC} \end{cases} \quad \begin{matrix} \\ \\ , i_o < i_{sc} \\ \\ , i_o \geq i_{sc} \end{matrix} \tag{2}$$

To account for the source's intrinsic dynamic behavior, the system incorporates transient operations driven by its internal capacitance and resistance. The statically estimated voltage is processed by a discrete-time first-order dynamic model that captures these internal parameters. Consequently, the total output voltage of the source encompassing the superposition of both the steady-state static response and the transient dynamic response is accurately calculated and defined by the third governing equation in this sequence. Unlike static models, the effective time constant is defined as a current-dependent piecewise function to capture transient asymmetry during rising and falling voltage transitions.

$$v_o(n) = v_o(n-1) + \frac{\Delta t}{\tau(I, \Delta I)} (v_o^{stat}(n) - v_o(n-1)) \tag{3}$$

It should be noted that Equation (3) and the formulated dynamic structure represent a proposed extension of the model. While the validation presented in this paper focuses primarily on the static and quasi-static mapping of power requirements, evaluating the corresponding transient responses remains a subject for future research.

The model's key ability to determine source temperature is seamlessly achieved through its multidimensional data structure. Instead of relying on computationally intensive iterative thermal equations, the internal temperature is obtained directly from table values using interpolation and extrapolation techniques. These techniques use thermal data derived from experiments performed on the energy source under different operating conditions, with the ambient temperature as a key input.

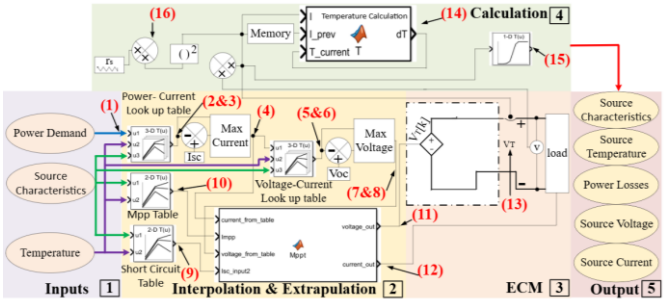

Fig. 1. UDCM Architecture

III. UDCM Validation

The validation of the proposed model was performed on two different PV technologies, monocrystalline and polycrystalline, in order to prove the robustness of the model in handling diverse PV technologies. The experimental data were acquired outdoors under stable environmental conditions, where the cell temperature remained almost constant.

A. Case Study 1: polycrystalline PV Module

The first examined cell was a polycrystalline solar cell, whose parameters are listed in Table 1. The model database was established using several experimental current–voltage (I–V) and current–power (P–I) measurements obtained under different irradiance levels of 495W/m² to 1030W/m².

TABLE I. POLYCRYSTALLINE PV PARAMETERS.

Rated output (Pmpp) at STC	Rated voltage (Vmpp) at STC	Open circuit voltage (Voc) at STC	Short circuit current (Isc) at STC	Cell temperature at STC	Rated current (Impp) at STC
100W	18.0V	21.6V	6.2	25°C	5.6A

The model was validated through a direct comparative analysis of experimental measurements and real-time simulation results at a solar irradiance level of 940 W/m². Crucially, this specific experimental profile was intentionally excluded from the model's initial training database to rigorously evaluate its generalization capability under untested operating conditions. As demonstrated by the operational curves (Fig. 2), the UDCM exhibits high-fidelity tracking up to the Maximum Power Point (MPP) region, where the simulated output closely aligns with the physical reality with MAE =0.92W, RMSE =3.7W, and APE =1.25%. Beyond the MPP threshold, the model successfully manages the cross-domain operational boundary, demonstrating only a minimal and stable deviation along the descending portion of the source's characteristic curves.

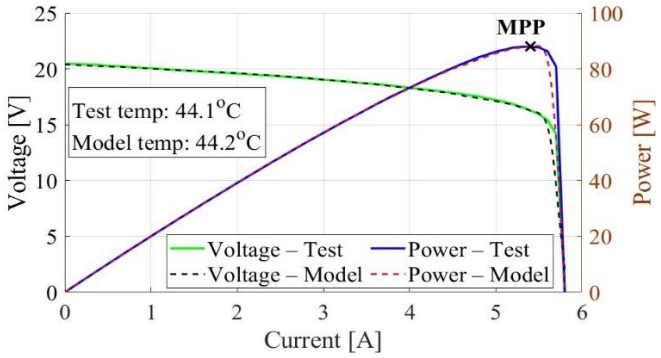

Fig. 2. Comparison Between Model Prediction and test Data at 940 $\frac{W}{m^2}$

B. Case Study 2: Monocrystalline PV Module

The second examined cell was a monocrystalline solar cell, whose parameters are listed in Table 2. The monocrystalline PV module has fundamentally different material chemistry, thermal behavior, and electrical properties compared to the baseline polycrystalline module, making it an ideal platform for testing technology-agnostic transferability. Throughout this evaluation, a comprehensive lookup database was established by mapping the source's characteristics across a range of operating envelopes. As shown in the experimental characteristic curves (Fig. 3), the measured peak power output reached approximately 35W under a lower solar irradiance of 460 W/m², scaling up significantly to a maximum of 68W under an elevated solar irradiance of 1019 W/m².

TABLE II. MONOCRYSTALLINE SP-5 PV PARAMETERS OF ONE CELL

Rated output (Pmpp) at STC	Rated voltage (Vmpp) at STC	Open circuit voltage (Voc) at STC	Short circuit current (Isc) at STC	Cell temperature at STC	Rated current (Impp) at STC
4.9W	16.9V	21.2V	0.31A	25°C	0.29A

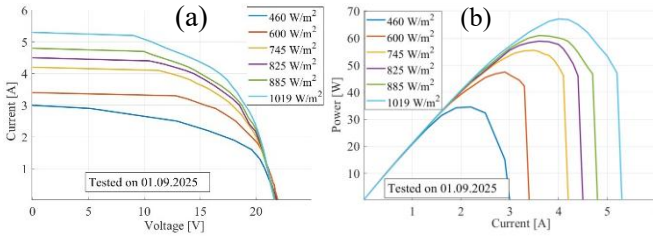

Fig. 3. SP-5 PV curves (a), voltage-current curves (b), power-current curves

To verify the accuracy and validity of the proposed model, verification points intentionally excluded from the model's original training database were examined. In Fig. 4, the model's runtime predictions at a solar irradiance level of 1007W/m² are presented alongside the actual experimental measurements for this specific point. An in-depth error analysis for this uncalibrated condition reveals the following statistical performance metrics, summarized in Table 3.

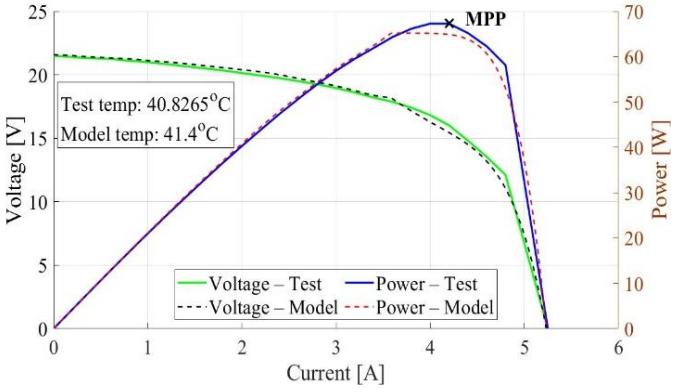

Fig. 4. Comparison Between Model Prediction and Test Data at 1007 $\frac{W}{m^2}$

TABLE III. PERFORMANCE METRICS: POWER PREDICTION ACCURACY AT 1007 W/M²

MAE [W]	RMSE [W]	MAPE (%)	R^2
0.7987	1.424	1.4	0.9963

To explicitly demonstrate the model's extrapolation capability beyond the trained dataset, an additional test case was evaluated at an extreme irradiance level of 1021 W/m². The extrapolated model predictions were directly compared to experimental measurements (Fig. 5), demonstrating that the linear extrapolation mechanism remained robust and highly accurate. For power estimation, the model achieved a RMSE of 1.9755W, a mean MAE of 1.0780W, and a mean MAPE of 1.93%, with a R^2 of 0.9923. Similarly, the voltage profile showed a strong agreement with the experimental data, yielding an RMSE of 0.4385V, an MAE of 0.2847V, a MAPE of 1.93%, and an R^2 of 0.9905. These metrics successfully validate the reliability and predictive fidelity of the UDCM framework when projecting energy source characteristics outside its validated baseline envelope.

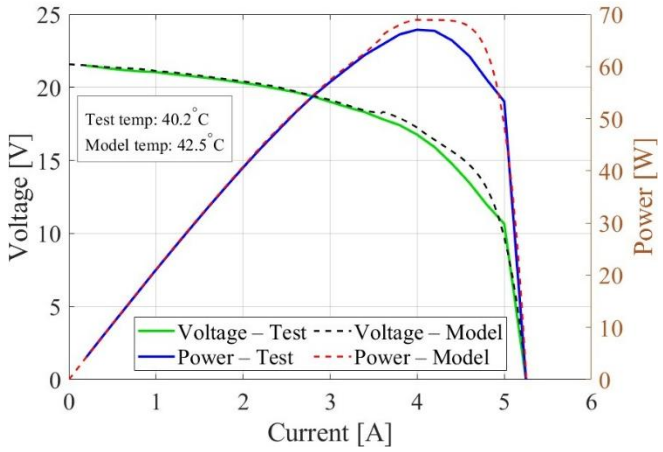

Fig. 5. Comparison Between Model Prediction and Test Data at 1021 $\frac{W}{m^2}$

Table IV. presents a comparative analysis between the proposed UDCM and the standard PV single-diode model, evaluating them based on accuracy and computational efficiency. The accuracy metrics for the standard single-diode model are derived from literature, showing an error of up to 5% against manufacturer NOCT data and climbing up to 10% when compared to experimental data [12]. In contrast, the proposed model significantly improves prediction accuracy, maintaining an APE/MAPE of less than 1.4% overall, with specific margins of 1.25% at 940W/m² and 1.4% at 1007 W/m². To evaluate computational speed, a direct simulation comparison was conducted in Simulink between the proposed and traditional models. These simulation results demonstrate that the proposed model optimizes efficiency by reducing the execution time by 30%, confirming its dual advantage in both fidelity and processing performance.

TABLE IV. COMPARISON OF THE PROPOSED UDCM WITH A STANDARD PV SINGLE-DIODE MODEL

	Accuracy (Error / MAPE)	Computational Performance
Single-diode model	Up to 5% error against manufacturer NOCT data, and up to 10% error against experimental data [12]	Baseline (x1)
The Proposed Model	APE/MAPE < 1.4% (1.25% at 940 W/m² and 1.4% at 1007 W/m²)	x1.43 Faster

IV. CONCLUSION

This paper presents a novel UDCM designed for the unified representation of diverse PV technologies. The proposed UDCM features a source-agnostic architecture that is directly driven by power demand rather than modeling the source based on its terminal voltage, as is common in traditional models, making it highly efficient where power demand-based scaling is required. By replacing rigid physical equations with an n-dimensional interpolation and extrapolation mapping system, the model performs deterministic, non-iterative calculations. By using deterministic logic instead of solving sets of coupled nonlinear equations, the model naturally eliminates the iterative convergence errors that often plague traditional network simulations. While the current study specifically validates this basic architecture at the individual module level, its non-iterative mathematical nature theoretically ensures absolute numerical stability for future large-scale configurations. The robustness of the framework was empirically validated using both monocrystalline and polycrystalline photovoltaic modules under untested environmental conditions. The experimental results demonstrated excellent tracking of physical measurements, achieving an APE below 1.4% and a coefficient of determination of up to 0.996. Ultimately, the UDCM provides a highly accurate, computationally efficient, and scalable solution for real-time performance optimization and load-power balancing in modern smart grids and microgrids.

ACKNOWLEDGMENT

This work made limited use of AI-based language tools to assist with text editing and concept clarification. All analyses, calculations, and final interpretations were independently performed and validated by the author.

REFERENCES

[1] X. Fang, S. Misra, G. Xue, and D. Yang, "Smart grid - The new and improved power grid: A survey," 2012. doi: 10.1109/SURV.2011.101911.00087.

[2] C. Wang and M. H. Nehrir, "Power management of a stand-alone wind/photovoltaic/fuel cell energy system," IEEE Transactions on Energy Conversion, vol. 23, no. 3, 2008, doi: 10.1109/TEC.2007.914200.

[3] S. S. S. R. Depuru, L. Wang, and V. Devabhaktuni, "Smart meters for power grid: Challenges, issues, advantages and status," 2011. doi: 10.1016/j.rser.2011.02.039.

[4] F. Blaabjerg, R. Teodorescu, M. Liserre, and A. V. Timbus, "Overview of control and grid synchronization for distributed power generation systems," 2006. doi: 10.1109/TIE.2006.881997.

[5] P. Palensky and D. Dietrich, "Demand side management: Demand response, intelligent energy systems, and smart loads," IEEE Trans. Industr. Inform., vol. 7, no. 3, 2011, doi: 10.1109/TII.2011.2158841.

[6] J. A. P. Lopes, C. L. Moreira, and A. G. Madureira, "Defining control strategies for microgrids islanded operation," IEEE Transactions on Power Systems, vol. 21, no. 2, 2006, doi: 10.1109/TPWRS.2006.873018.

[7] M. G. Villalva, J. R. Gazoli, and E. R. Filho, "Comprehensive approach to modeling and simulation of photovoltaic arrays," IEEE Trans. Power Electron., vol. 24, no. 5, 2009, doi: 10.1109/TPEL.2009.2013862.

[8] S. Li, H. He, C. Su, and P. Zhao, "Data driven battery modeling and management method with aging phenomenon considered," Appl. Energy, vol. 275, 2020, doi: 10.1016/j.apenergy.2020.115340.

[9] N. Guruwacharya, S. Chakraborty, G. Saraswat, R. Bryce, T. M. Hansen, and R. Tonkoski, "Data-Driven Modeling of Grid-Forming Inverter Dynamics Using Power Hardware-in-the-Loop Experimentation," IEEE Access, vol. 12, 2024, doi: 10.1109/ACCESS.2024.3383323.

[10] K. Ishaque, Z. Salam, and H. Taheri, "Simple, fast and accurate two-diode model for photovoltaic modules," Solar Energy Materials and Solar Cells, vol. 95, no. 2, 2011, doi: 10.1016/j.solmat.2010.09.023.

[11] H. Jayasinghe, K. Gunawardane, and R. Nicholson, "Applications of Electrical Load Modelling in Digital Twins of Power Systems," 2025. doi: 10.3390/en18040775.

[12] S. A. Rahman, R. K. Varma, and T. Vanderheide, "Generalised model of a photovoltaic panel," IET Renewable Power Generation, vol. 8, no. 3, 2014, doi: 10.1049/iet-rpg.2013.0094.